Composites

CrossMark

Composites with surface-grafted cellulose nanocrystals (CNC)

Lilian Forsgren[1] , Karin Sahlin-Sjövold[2,3] , Abhijit Venkatesh[1] , Johannes Thunberg[1] ,
Roland Kádár[1,3] , Antal Boldizar[1,3] , Gunnar Westman[2,3,*] , and Mikael Rigdahl[1,3]

[1] Department of Industrial and Materials Science, Chalmers University of Technology, 412 96 Gothenburg, Sweden
[2] Department of Chemistry and Chemical Engineering, Chalmers University of Technology, 412 96 Gothenburg, Sweden
[3] Wallenberg Wood Science Center, Chalmers University of Technology, 412 96 Gothenburg, Sweden

ABSTRACT

Hydroxyazetidinium salts were used to surface-modify cellulose nanocrystals (CNC) by grafting the salts onto the sulphate ester groups on the CNC surfaces. The grafting was confirmed by ζ-potential measurements and by the thermal degradation behaviour of the modified CNC. The thermal stability (onset of degradation) of the CNC was improved by the surface modification (almost 100 °C). Composites containing surface-modified or unmodified CNC (0.1, 1.0 and 10 wt%) with an ethylene-based copolymer as matrix were produced by compression moulding. The thermal stability of the composites was not, however, markedly improved by the surface grafting onto the CNC. It is suggested that this is due to a degrafting mechanism, associated with the alkaline character of the system, taking place at high temperatures. Model experiments indicated, however, that this did not occur at the conditions under which the composites were produced. Furthermore, in the case of a reference based on pH-neutralised polymeric system and modified CNC, an upward shift in the onset of thermal degradation of the composite was observed. The addition of the CNC to the polymer matrix had a strong influence of the mechanical performance. For example, the tensile modulus increased approximately three times for some systems when adding 10 wt% CNC. The surface grafting of the hydroxyazetidinium salts appeared mainly to affect, in a positive sense, the yield behaviour and ductility of the composites. The results of the mechanical testing are discussed in terms of interactions between the grafted units and the matrix material and between the grafted groups.

Address correspondence to E-mail: westman@chalmers.se

⚉ Springer

Introduction

There is a growing demand for a reduction in the use of fossil-based materials and for the development of stronger lightweight materials that could reduce the amount of material needed and provide lighter structures. Polymer composites containing wood-based or cellulose-based materials as fillers/reinforcing elements are obvious candidates here. The idea of using such materials is certainly not new (see e.g. [1–5]). Cellulose fibres provide some important benefits in this context (see also Pickering et al. [6]): low density, good specific mechanical properties, availability in large volumes, renewability, biodegradability and low abrasion towards processing equipment. The drawbacks associated with such fibres in thermoplastic matrices are well known and include, for instance, limited adhesion between the hydrophilic fibres and, in most cases, the hydrophobic nature of the polymer matrix, the poor dispersion of the fibres in the matrix, and the moisture uptake and degradation of the fibres at the temperatures used for thermoplastic forming. Some of these drawbacks can be reduced by chemical modification of the fibres and/or by using compatibilisers/coupling agents (see e.g. [7–10]), but improvements are still desired.

During recent years, interest in using cellulose nanomaterials in the form of cellulose nanofibrils (CNF) and/or cellulose nanocrystals (CNC) as reinforcing elements in polymer matrices has increased quite drastically, due to the potentially good mechanical properties (modulus and strength) of these materials. Both CNF and CNC are thin, of the order of 10 nm, but the CNF are significantly longer, up to the µm range, whereas CNC have a length of approximately 200 nm. The CNF can be obtained from cellulose fibres using an aqueous homogenisation process, often combined with a pre-treatment of the fibres. The CNC are produced by acid hydrolysis of cellulose fibres or fibrils (see e.g. Beck-Candanedo et al. [11]), which to a great extent removes the non-ordered parts of the fibre leaving rod-like elements with an enhanced crystallinity. Both types of reinforcing materials have in several reports been shown to significantly improve the mechanical performance when incorporated into a polymeric matrix [12–20], although it is difficult to compare the results since differences in the type of original fibres used as well as in the preparation and processing methods have

an effect on the final composite performance. It is, however, of interest to note that Xu et al. [15] used both CNF and CNC in the same matrix (polyethylene oxide) and found that CNF was somewhat more effective than CNC with regard to improvement in stiffness, strength and toughness. This result was suggested to be an effect of the larger aspect ratio of the CNF.

Here, interest is focused on CNC as reinforcing element motivated by their greater crystallinity and the expected less tendency for entanglement into aggregates. From a literature study, Lee et al. [17] estimated the axial tensile modulus of crystalline cellulose to be between 58 and 180 GPa, and the tensile strength to be between 0.3 and 22 GPa, indicating that CNC should surely provide good as reinforcement of polymers. The less entangled structure allows for higher concentrations in the dispersions and should promote the processing properties of CNC composites compared to those containing CNF.

In the present work, sulphuric acid was used in the hydrolysis of the cellulose to obtain CNC. As reported by Beck-Candanedo et al. [11], this treatment converts some of the hydroxyl groups on the surface of the CNC to negatively charged sulphate ester groups which increase the stability of water-based CNC dispersions. However, the presence of acid sulphate groups reduces the thermal stability of the nanocellulose, and thermal degradation, which has been attributed to a dehydration reaction [21, 22], may commence already at 150 °C. In an earlier work [23], it was shown that the onset of thermal degradation of CNC obtained through sulphuric acid hydrolysis could be delayed by almost 100 °C by grafting azetidinium salts onto the sulphate ester groups on the CNC surface. Sahlin et al. [23] used three different chemical groups to modify the CNC; *N*-morpholino-3-methoxyazetidinium, *N,N*-dihexyl-3- methoxyazetidinium and *N,N*-diallyl-3-methoxyazetidinium. In addition to the improvement in thermal stability, the surface modifications of the CNC resulted in a significant increase in the shear viscosity at a given shear rate and in the dynamic moduli of aqueous dispersions containing 0.65 and 1.3 wt% CNC, and there was a corresponding decrease in the concentration at which gel formation took place. It was suggested that this influence of the surface treatment of the CNC on the rheological

behaviour could be associated with hydrophobic attractive interactions between the grafted groups.

Sahlin et al. [23] indicated that a surface treatment of this kind can constitute a starting point for enhancing the dispersion of the reinforcing elements in the polymer matrix and increase the mechanical performance of such polymer composites by increasing the compatibility between the constituents of the composites. Börjesson et al. [24] recently described CNC composites in which azetidinium salts with carbon dialkyl substituents were grafted onto the CNC surfaces. These particles were then incorporated (about 3 wt%) into a low-density polyethylene matrix using a mini-extruder. The positive influence of the surface treatment on the thermal stability of the composites compared with that of the composite containing non-treated CNC was confirmed, but no positive effect on the mechanical properties that could be associated with the surface treatment was established.

In the present work, the CNC were surface-treated by grafting N-morpholino-3-hydroxyazetidinium, N,N-dihexyl-3-hydroxyazetidinium or N,N-diallyl-3-hydroxyazetidinium onto the surface of the nanocrystals. The mechanical performance, thermal properties and thermal stability of polymer composites based on these surface-treated CNC and poly(-ethylene-co-acrylic acid) copolymer (EAA) as the matrix were evaluated. The use of EAA as the matrix was motivated by its compatibility with cellulose, as indicated by the increase in strength when cellulose fibres were added to EAA [25]. Three different concentrations of CNC in the composite materials were used, 0.1, 1.0 and 10 wt%. The composites were manufactured by compression moulding of dried mixtures of CNC and EAA.

Experimental

Materials

Aqueous dispersions of untreated CNC were obtained by the acid hydrolysis of microcrystalline cellulose using a procedure (with some modifications) outlined by Hasani et al. [26]. The process has been described in detail by Sahlin et al. [23]. In a previous work, Moberg et al. [27], using atomic force microscopy, estimated the average length and width

of CNC units, prepared in a similar manner, to be 211 ± 114 nm and 6.0 ± 1.5 nm, respectively.

As stated in the "Introduction" section, the CNC were surface-treated by grafting N-morpholino-3-hydroxyazetidinium, N,N-dihexyl-3-hydroxyazetidinium or N,N-diallyl-3-hydroxyazetidinium onto the surface of the nanocrystals. These modified CNC are hereinafter denoted CNC-Morph-OH, CNC-diHexyl-OH and CNC-diAllyl-OH. The grafting of the chemical groups followed an improved version of a method described in Ref. [23], which was based on a procedure outlined by Chattopadhyay et al. [28]. The azetidinium salts were synthesised as described by Sahlin et al. [23], except that, in the present study, the methylation of the azetidinium salts was omitted. The hydroxyazetidinium salts were mixed with the aqueous CNC suspension (0.1 mol equiv hydroxyazetidinium salt/anhydrous glucose unit) in a round-bottomed flask and stirred vigorously. When a good mixing of the salt and CNC had been achieved, the mixture was heated to 90 °C and stirred for 22 h. The reaction mixture was then allowed to cool to room temperature and subsequently washed with acetonitrile and ethanol, and finally deionised water using repeated centrifugation steps. The modified CNC were characterised by ζ-potential measurements and thermal gravimetric analysis.

The EAA copolymer, obtained from BIM Kemi AB, Sweden, was used as a dispersion with a 20 wt% solids content at pH 9.7. According to the supplier, the acrylic acid content of the polymer was 15%, its melting point and density were 88 °C and 0.994 g/cm^3, respectively, and the melt flow rate was 36 g/10 min (ISO 1133, 190 °C, 2.16 kg).

Production of composites

The aqueous dispersions of CNC (modified and unmodified) and EAA were mixed in different proportions in order to obtain targeted weight fractions of CNC in the composites of 0.1, 1 and 10 wt%, corresponding to volume fractions of 0.066, 0.67 and 6.85% assuming a density of 1.5 g/cm^3 of dry CNC. Rheological measurement on aqueous dispersions of CNC surface-modified by similar, but not identical, salts indicated that the percolation threshold was below 0.5 wt%, whereas in the case of the unmodified CNC, it was about 2.5 wt% [23]. The mixing was performed with an IKA T25 digital Ultra Turrax at a rotational speed of 7400 rpm for 6 min. The mixed

dispersions were dried in air at room temperature for approximately 1 week to form sheets. Then, 12 g of the dried material was compression-moulded into square plates 100×100 mm^2 in size with a thickness of about 1 mm. The compression moulding was performed with a Bucher-Guyer KHL 100, Switzerland, about 12 g of material being placed in the mould at 105 °C. A low pressure of 20 bar was applied, allowing for pre-heating, until the distance between the mould halves had stabilised, which took about 5 min. A pressure of 500 bar was then applied and the mould was cooled to 30 °C, which took 3–4 min. The cooling of the mould was then stopped, allowing the mould temperature to recover to 40 °C, which took about 1 min. The pressure was then released, and the sample was removed from the mould.

A pH-neutral composite was also prepared on a smaller scale by ion exchange. The EAA dispersion was first mixed with ion exchange resin (Dowex® Marathon™ MR-3 hydrogen and hydroxide), and CNC-diAllyl-OH was then added to a target weight fraction of 10 wt%. The mixture was stirred for 4 h, followed by removal of the ion exchange resin by centrifugation, and subsequently dried at room temperature. The composite material was then produced by compression of the dry mixture at 105 °C at 5 bar for 5 min.

Characterisation methods

ζ-Potential

The ζ-potential of all the CNC samples was measured using a Zetasizer Nano ZS (Malvern Instruments, UK) based on the laser Doppler velocimetry technique. The light source was a 50 mW diode-pumped solid-state laser with a wavelength of 532 nm. All measurements were taken at 25 °C using DTS1070 disposable folded capillary cells. The samples were stabilised for 120 s inside the device, and five measurements per sample were recorded with 5 runs per measurement on three replicates. Samples were prepared by dilution to 0.05 wt% dry content and ion exchanged (Dowex® Marathon™ MR-3 hydrogen and hydroxide) overnight followed by subsequent removal of resin beads by filtration prior to the measurement.

Thermal gravimetric analysis (TGA)

The onset of thermal degradation of the CNC as well as of the CNC-containing composites containing 10 wt% nanocrystals was determined using a TGA/DSC 3+ Star system (Mettler Toledo, Switzerland). The specimens (about 10 mg) were subjected to a heating ramp of 5 °C/min between 25 and 550 °C under nitrogen at a flow rate of 50 mL/min.

Visual assessment of the thermal stability

In order to obtain a visual impression of the thermal stability of the composites, small samples of each composite containing 10 wt% of CNC were placed at five different temperatures on a Kofler Bench that provided a heat gradient. Samples were placed at 120, 130, 140, 150 and 160 °C for 8 min, to determine at which temperature discoloration of the composite took place and hence maybe also when the thermal degradation was initiated for the different CNC composites as well as for the unfilled EAA.

Mechanical properties

Tensile test bars with a gauge length of 40 mm were cut from the compression-moulded plates and kept in a conditioned environment at 25 °C and 55% relative humidity for at least 4 days before performing the tensile tests. The tensile properties (Young's modulus, tensile strength at yield, elongation at yield, tensile strength at break and elongation at break) were measured at 25 °C with a strain rate of 2.5×10^{-3} s^{-1} (6 mm/min) using a Zwick/Z2.5 tensile tester with a 500 N load cell. The reported values are in most cases the average values of six independent measurements.

Dynamic-mechanical analysis

The dynamic-mechanical properties were measured using a Rheometrics RSA II at room temperature (25 °C) at a frequency of 1 Hz. The specimens were pre-strained to a strain of about 0.15% (in tension), which was kept constant during the measurements and a sinusoidal deformation was superimposed. During the test, the strain amplitude of the sinusoidal deformation was increased from about 0.03–0.14%.

It is known that surface treatment of filler particles can affect the mechanical loss factor of a composite

material and such effects can be associated with, for example, polymer–filler particle friction or poor adhesion between the reinforcing element and the matrix (see also Nielsen [29]). Interactions at the interface between the added particles and the polymer can lead to the formation of an interphase region in the matrix, close to the filler particles, with properties different from those of the bulk polymer. As a starting point, the influence of the interphase region on the mechanical loss factor of the composite (tan δ_c) can be written as [30]

$$\tan \delta_c = v_f \tan \delta_f + v_i \tan \delta_i + v_m \tan \delta_m \quad (1)$$

where the subscripts f, i and m refer to the filler, the interphase region and the polymer matrix, respectively, and v denotes the corresponding volume fractions. As pointed out [30], Eq. (1) is probably an oversimplification of the mechanical damping of a polymer composite, but it can be useful when a more detailed understanding of the influence of different surface treatments on the mechanical coupling between the filler and the matrix is being sought. Intuitively, it is probable that the loss factor increases if the interphase region is weak, due, for example, to a poor degree of adhesion between the phases, promoting friction losses during the imposed sinusoidal deformation.

Differential scanning calorimetry (DSC)

DSC using a Perkin-Elmer DSC7 was employed to assess the thermal transitions and the crystallinity of the composite materials. The endotherms were recorded in a nitrogen atmosphere, while the temperature was increased from − 20 to 150 °C at a scan rate of 10 °C/min. No second temperature scan was used. The crystallinity (X_c) was evaluated as

$$X_c = \frac{\Delta H_c}{w_{EAA} \Delta H_o} \quad (2)$$

where ΔH_c is the specific heat of fusion of the composite, w_{EAA} the weight fraction of EAA and ΔH_o the specific heat of fusion for 100% crystalline polyethylene, 277.1 J/g [31].

Results and discussion

CNC characterisation

The unmodified CNC have been extensively characterised in a previous paper [23]. In the present study, ζ-potential measurements and TGA were used to confirm that grafting had taken place. The decrease in surface charge and the increase in thermal stability, shown in Table 1, suggest that grafting of the azetidinium salts was successful, although the CNC-Morph-OH seems to have a somewhat lower degree of substitution.

Manufacturing procedure

Aqueous dispersions of CNC and EAA were mixed followed by a drying phase in order to minimise the tendency towards aggregation of the CNC particles and thus obtain well-dispersed CNC in the composite materials (see also Venkatesh et al. [32]). Visual inspection of the compression-moulded plaques revealed no aggregates in the samples. The plaques were more or less transparent, even up to a concentration of 10 wt% CNC but with some differences in colour, as can be seen in Fig. 1.

The composite containing 10 wt% CNC-Morph-OH behaved somewhat differently from the other two composites and had a more yellowish appearance and somewhat more visible defects. The discoloration of the CNC-Morph-OH was not further investigated, but there are reports and studies of the influence of amine structure on the yellowing [33, 34]. The CNC-diHexyl-OH and CNC-diAllyl-OH composites were colourless, and their visual appearance was very close to that of the composite containing the untreated CNC and also the unfilled EAA plaque.
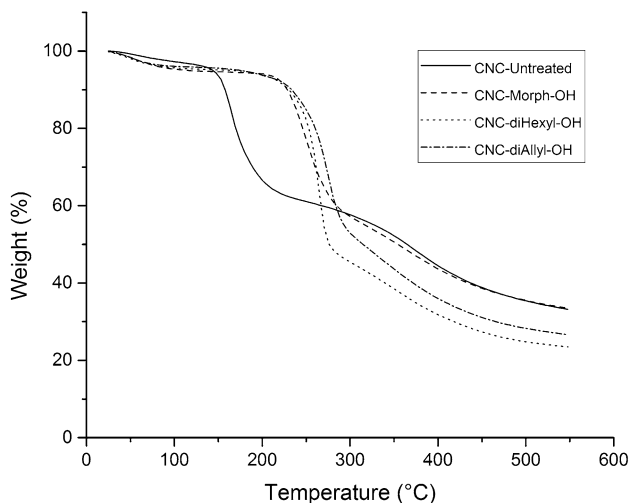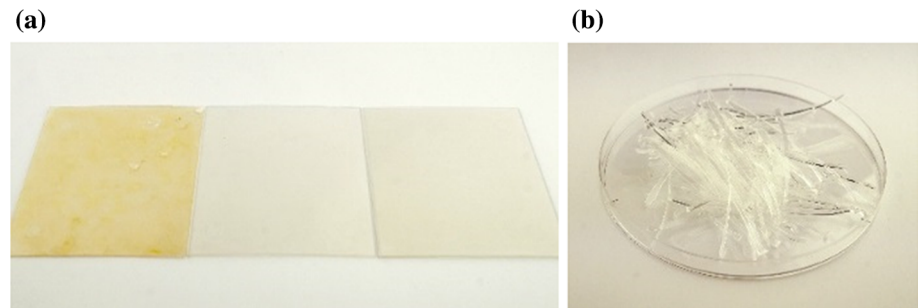
Thermal stability

Thermal gravimetric analysis, TGA, of the modified CNC showed an increase in the onset temperature by thermal degradation of almost 100 °C compared to that of the unmodified CNC, as shown in Table 1 and Fig. 2. This can be attributed to the conjugation with the sulphate half ester, which removed the acidic hydrogen associated with the sulphate half ester, thus preventing the catalysed degradation (see also [22, 23])

Table 1 ζ-Potential (standard deviation in parentheses) of ion-exchanged CNC at a concentration of 0.05 wt%, the onset of thermal degradation and the weight percentage of residual char at 550 °C
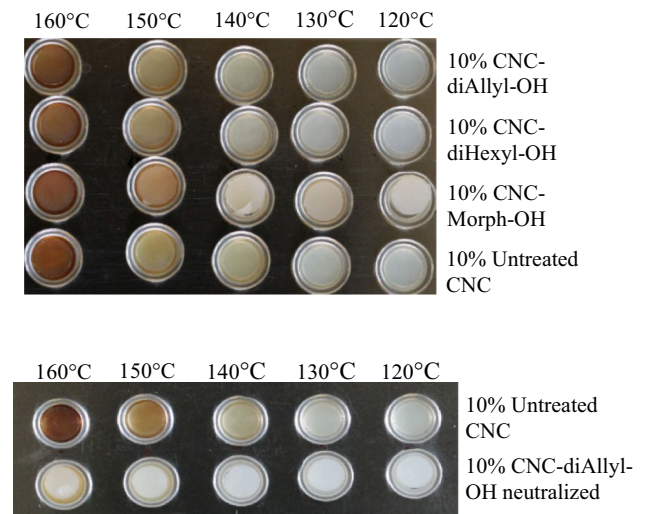
Type of CNC	ζ-Potential (mV)	T_{onset} (°C)	Residual char (%)
CNC-unmod.	− 71.7 (2.0)	157	32
CNC-Morph-OH	− 40.9 (1.1)	224	33
CNC-diHexyl-OH	− 32.5 (2.5)	248	23
CNC-diAllyl-OH	− 31.0 (2.1)	247	27

Figure 1 **a** Composites with 10 wt% CNC, from left; CNC-Morph-OH, CNC-diHexyl-OH and CNC-diAllyl-OH, **b** dried composite material, with 1 wt% CNC-diAllyl-OH before compression moulding.

Figure 2 Thermogravimetric curves showing the thermal degradation of untreated and surface-modified CNC.

Figure 3 Upper photograph: visual appearance of the composites containing 10 wt% CNC after exposure for 8 min to (from right to left) 120, 130, 140, 150 and 160 °C. Lower photograph: visual appearance of the composites containing 10 wt% untreated CNC and 10 wt% CNC-diAllyl-OH from the pH-neutralised system after exposure for 8 min to (from right to left) 120, 130, 140, 150 and 160 °C.

TGA measurements together with a visual assessment were used to study the thermal stability of the composites containing 10 wt% CNC. Figure 3 shows the appearance of the composites containing 10 wt% CNC after exposure to (from right to left) 120, 130, 140, 150 and 160 °C for 8 min. At 150 °C, the colour started to change, and at 160 °C, all the samples were quite brownish. No significant difference between the composites could be detected, i.e. the functional groups grafted onto the CNC did not increase the visual thermal stability of these EAA-based composites. A similar experiment with unfilled EAA did not reveal any colour change at all up to 160 °C, i.e. the samples remained transparent. Figure 3 also

includes images of the pH-neutral composites containing CNC-diAllyl-OH. No significant colour change was noted up to 160 °C for this composite.

The TGA results (Fig. 4) showed similarly that, regardless of the type of modification or lack thereof, the thermal degradation of the composites was initiated at ca 150 °C (with the exception of the pH-neutralised composite). This was somewhat surprising since the TGA of the modified CNC showed thermal
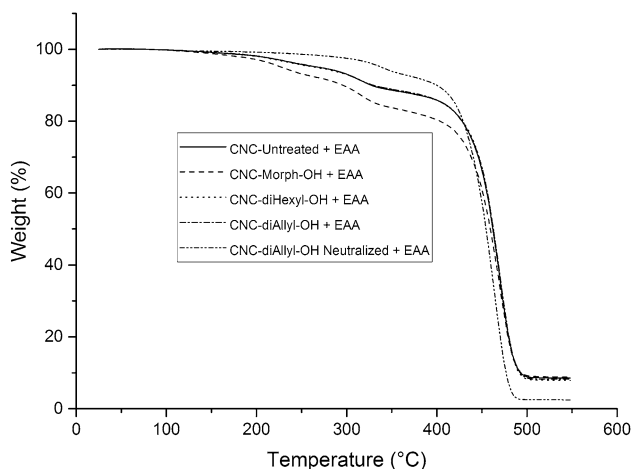
Figure 4 Thermogravimetric curves showing the thermal degradation of the composites containing 10 wt% of the surface-modified CNC. The curve for the composite based on a neutralised mixture of EAA and CNC-diAllyl-OH (10 wt%) is also included.

stability up to ca 250 °C (see Fig. 2). The explanation may be found in the chemical stability of the sulphate diester. It is well established within organic chemistry that sulphates act as good leaving groups in the presence of a nucleophile, such as hydroxide and carboxylate, which is abundant at pH 9.7 (the pH level of the EAA dispersion). As a consequence, the azetidinium groups on the sulphate diesters are cleaved by the carboxylates of the EAA matrix, generating sulphate half-esters that have lower thermal stability. At neutral pH, where the carboxylate is in the carboxylic acid form and thus less reactive, it is less prone to react with the sulphate diester; thus, no degradation at 150 °C is observed.

In order to verify the hypothesis that the reduction in thermal stability was in fact caused by the alkalinity of the polymer dispersion, a composite was prepared from a neutralised mixture of EAA dispersion and 10 wt% CNC-diAllyl-OH. The TGA curve for this composite, included in Fig. 4, did not reveal any sign of the early onset of thermal degradation at 150 °C, supporting the hypothesis that the alkalinity was responsible for the decreased stability of the azetidinium-grafted CNC composites. When the cause of the early degradation had been identified, it was important to establish that the grafting remained after the composites had been processed. Since it was not possible to observe the characteristic peaks of the CNC nor of the linker with FTIR (Fourier transform infrared spectroscopy), an indirect method was employed. CNC-diAllyl-OH was pH-adjusted to

pH 9.7, dried at room temperature and then pressed at 105 °C at 5 bar for 5 min. FTIR spectra and TGA curves were obtained before and after the heating, and they showed no differences. It was therefore concluded that neither the mixing nor the processing at 105 °C was likely to have caused degrafting and that higher temperatures are required to degraft at the alkalinity of these composites.

Mechanical properties of the CNC composites

At the lower concentrations of CNC (0.1 and 1 wt%), all the samples exhibited a clear yield point followed by a cold-drawing behaviour. An example of this in the case of CNC-diAllyl-OH (1 wt%) is given in Fig. 5 where the typical experimental scatter is also illustrated. At a CNC content of 10 wt%, the yielding phenomenon was less pronounced and the ductility of the composites decreased quite dramatically. In some cases, with the highest CNC content, it was difficult to assign a yield point during the tensile test. This was most evident in the case of the composite containing 10 wt% unmodified CNC for which no yield point could be determined in an unambiguous way. When discussing the ultimate properties of the composites, attention is focussed more on the yielding behaviour, since in the case of ductile polymeric systems, this is usually of more interest in design of
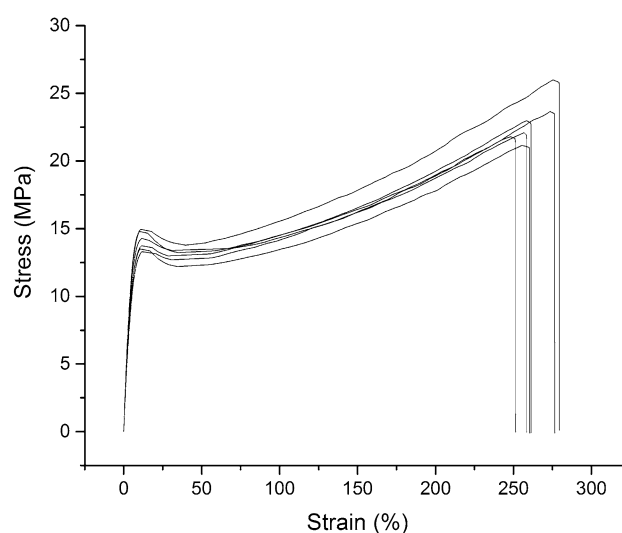

Figure 5 Tensile stress–strain behaviour of the CNC-diAllyl-OH composite (1 wt% CNC). The different curves refer to different tests and illustrate the experimental scatter.

different components than the ultimate failure of the system which may occur at very large deformations.

The results of the tensile tests are summarised in Table 2. It is evident in Fig. 6 that the incorporation of the CNC has a very strong positive effect on the tensile modulus, E, of the polymeric materials, even at these quite low CNC contents. The modulus increases from ca 300 MPa up to more than 900 MPa when the material is reinforced with 10 wt% unmodified CNC (less than 7 vol% CNC). This increase is discussed in more detail in the next section.

At low CNC contents, the materials containing CNC-Morph-OH appeared to be somewhat more effective in improving the modulus than the other CNC (although the differences are not large). But this was not the case at a CNC content of 10 wt%, where this treatment produced the lowest E-value, partly due perhaps to the appearance of defects as stated previously (Fig. 1). At 10 wt%, the highest tensile modulus was obtained with the untreated CNC, closely followed by CNC-diAllyl-OH. A general observation relating to the CNC contents of 1 and 10 wt% is that the surface treatment of the nanocellulose may have resulted in a somewhat more flexible (softer) material, possibly related to interactions between the grafted groups and the polymer matrix leading to the formation of an interphase region with properties different from that of the EAA matrix. This is further discussed in some detail at the end of this section.
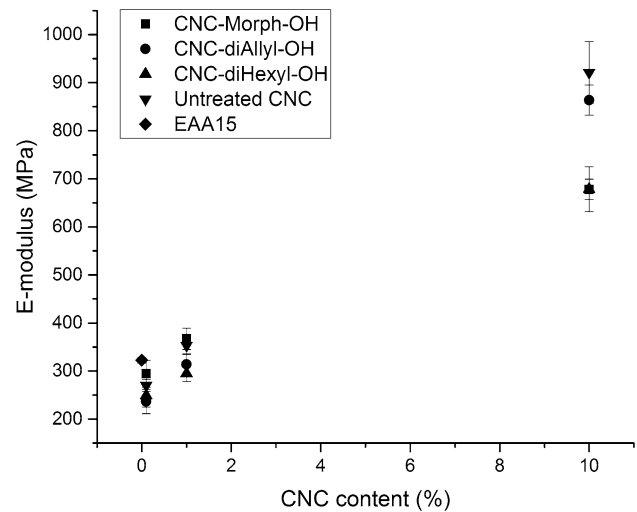
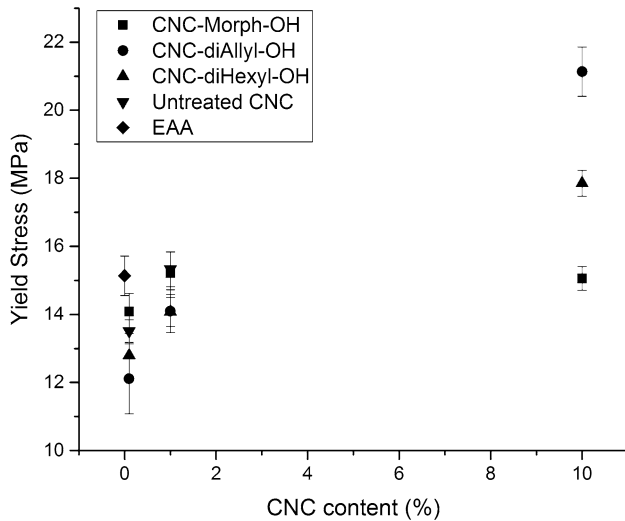**Figure 6** Elastic modulus of the composites as a function of the CNC content.

The yield stress, σ_y, exhibited in a sense the same behaviour as the modulus, i e. the highest σ_y-values were noted for CNC-Morph-OH at a low CNC content, but the CNC-diAllyl-OH exhibited the highest yield stress at a CNC content of 10 wt% (see Fig. 7) which, as suggested earlier, may be related to defects appearing in the 10 wt% CNC-Morph-OH. No clear yield point could be assessed for the composite containing 10 wt% untreated CNC. In all cases, however, the inclusion of the cellulosic nanocrystals led to an increase in the yield stress of the material. This is a positive result, since the incorporation of a rigid filler

Table 2 Mechanical properties of the CNC composites

Material	Modulus (MPa)	Yield stress (MPa)	Yield strain (%)	Failure stress (MPa)	Failure strain (%)
0.1% CNC-Morph-OH	294 (28)	14.1 (0.5)	10.4 (0.6)	24.3 (0.8)	284 (11)
0.1% CNC-diAllyl-OH	237 (25)	12.1 (1.0)	12.2 (0.4)	21.2 (1.3)	276 (11)
0.1% CNC-diHexyl-OH	249 (24)	12.8 (0.6)	12.0 (0.8)	23.5 (1.4)	288 (15)
0.1% untreated CNC	270 (13)	13.5 (0.3)	11.4 (0.8)	24.5 (0.7)	278 (6)
1% CNC-Morph-OH	367 (22)	15.2 (0.6)	10.2 (0.4)	23.4 (1.3)	252 (10)
1% CNC-diAllyl-OH	314 (21)	14.1 (0.6)	11.0 (0.5)	22.9 (1.0)	261 (10)
1% CNC-diHexyl-OH	295 (16)	14.1 (0.4)	11.7 (0.9)	23.7 (1.2)	267 (10)
1% untreated CNC	353 (18)	15.3 (0.5)	9.9 (0.2)	25.3 (1.7)	246 (7)
10% CNC-Morph-OH	678 (46)	15.1 (0.4)	7.5 (0.4)	14.2 (2.3)	11 (10)
10% CNC-diAllyl-OH	864 (32)	21.1 (0.7)	8.2 (0.8)	19.7 (0.8)	31 (22)
10% CNC-diHexyl-OH	678 (21)	17.9 (0.4)	8.6 (0.7)	16.5 (1.0)	28 (15)
10% untreated CNC	921 (64)	–	–	21.9 (0.9)	6 (1)
EAA	322 (5)	15.1 (0.6)	9.6 (0.6)	25.8 (1.2)	255 (6)

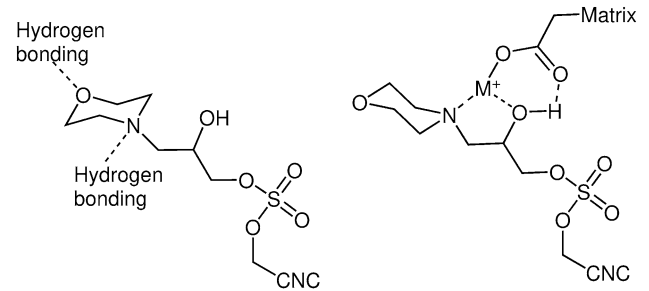The average values are given with standard deviation in parentheses

Figure 7 Yield stress of the composites as a function of the CNC content.

Figure 8 Schematic presentation of possible interactions between the matrix and CNC-Morph-OH. To the left, the hydrogen bonds to water and hydroxyl and carboxylate in the matrix are indicated. To the right, a chelate between morpholine substituent and matrix is shown where $M^+=H$ or Na^+.

often reduces the ultimate stress of a composites (see also Nielsen [29]).

The strain at the yield point was in fact increased by the addition of 0.1 and 1 wt% CNC (see Table 2). In general, it appears that the surface treatment increased the ductility of the composite compared with that of the composite containing the untreated CNC. This is also reflected in the strain at break of the composites, especially with a CNC content of 10 wt% (Table 2). The composite containing 10 wt% untreated CNC had the lowest elongation at break of only 6%. As mentioned earlier, the enhanced ductility of the composite material may be due to an interaction between the grafted chemical groups and the polymer matrix.

The way in which the surface groups affect the mechanical properties of the composites is rather complex. At 0.1 and 1 wt%, rather close to the expected percolation threshold of the CNC network, it can be assumed that there is negligible or minor aggregation of the nanocrystals, usually through OH interactions. Thus, the mechanical properties are due mainly to the presence of the CNC and possible interactions of the surface groups with themselves or with the polymer matrix. For the dihexyl groups, hydrophobic interactions can be assumed, for the diallyl π–π interactions and for the morpholine substituent and for the unsubstituted CNC hydrogen bonding, possibly assisted by residual water molecules. The possible hydrogen bonding sites of morpholine are schematically shown in Fig. 8 (left part of

the figure). It is interesting that CNC-Morph-OH gave the greatest improvement in mechanical behaviour at the lower CNC contents, implying that there are pronounced interactions either between crystals or between the crystals and the matrix, presumably because, compared to the other derivatives, morpholine-substituted CNC have a greater tendency to interact with the carboxylate groups in the matrix as shown schematically in Fig. 8 ($M^+=H$ or Na^+ in the picture to the right).

At 10 wt%, there are stronger interactions, since the larger amount of CNC results in a great contact (interfacial) area, and other factors may affect the structural-mechanical relationship. In the untreated CNC, the hydrogen bonding between sulphate groups and hydroxyl groups has a strong affect, but in the substituted CNC this effect is negligible. In the case of the substituted CNC, the diallyl substituents seem to have a stronger effect on the mechanical properties than the morpholine and dihexyl substituents. Whether this is due to a "good size and match" between the linkers at 10 wt% or because the π–π interactions are stronger than the van der Waals interaction between the dihexyl substituents needs a more thorough investigation. At the highest CNC content, aggregation of the CNC particles may lead to interactions between the grafted substituents on different CNC particles and to interactions between the surface groups and the matrix which affect the mechanical properties, due to the formation or existence of interphase regions in the composite material.

Estimation of the tensile modulus of the CNC

A simple model to estimate the axial tensile modulus of the CNC (E_f) is that of Cox–Krenchel (see also [17, 35, 36]).

$$E_c = \eta_L \eta_O f E_f + (1-f) E_m \quad (3)$$

where E_c is the measured tensile modulus of the composite (given in Table 2), E_f the modulus of the CNC, E_m the tensile modulus of the EAA matrix (given in Table 2 being 322 MPa) and f the volume fraction of the CNC. The factor η_o accounts for the orientation of the nanocrystals, and assuming that the crystals are randomly distributed in the plane, it has the value 3/8 [35]. The effect of the finite length of the nanocrystals is reflected in the factor η_L which can be expressed using the shear lag theory as [36]

$$\eta_L = 1 - \frac{\tanh(na)}{na} \quad (4)$$

with

$$n = \sqrt{\frac{2G_m}{E_f \ln\left(\frac{2R}{d}\right)}} \quad (5)$$

and where a is the aspect ratio of the CNC. Using the data reported by Moberg et al. [27], the aspect ratio was estimated to be 210/6 = 35. The shear modulus G_m of the matrix can be obtained from the tensile modulus of the unfilled EAA. In Eq. (5), $2R$ is the distance between the nanocrystals and d the diameter of CNC. Assuming that the crystals are positioned in a square array, the ratio R/d can be calculated from the volume fraction f of the nanocrystals.

Using the tensile moduli given in Table 2 for the EAA matrix and for the composite containing 10 wt% untreated CNC (assuming perfect adhesion between the matrix and the CNC), the modulus of the CNC can be estimated to be 55–60 GPa. This is certainly a high value, approaching that of glass fibres which have a value of ca 70 GPa. It is also higher than or similar to the values reported for the effective modulus of cellulose nanofibrils, for example 29–36 GPa [37], 33–62 GPa [16] and 25–42 GPa [18].

Dynamic-mechanical analysis

Figure 9 shows the mechanical loss factor as a function of the applied strain amplitude for the composites containing untreated CNC and for unfilled EAA.
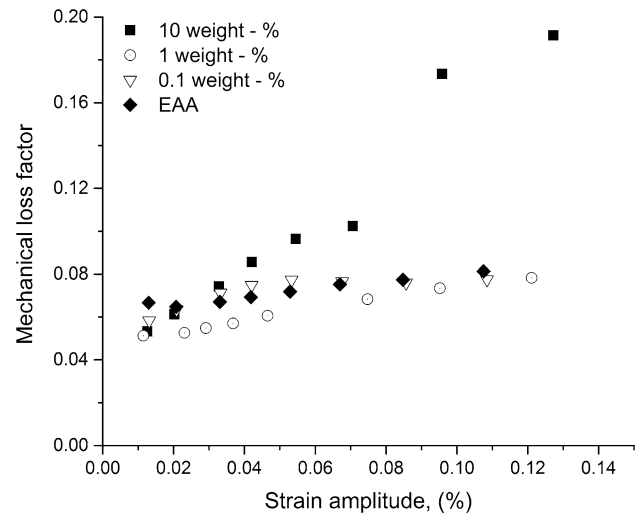
Figure 9 Mechanical loss factor as a function of the applied strain amplitude. The composites contained 0 (denoted EAA), 0.10, 1 and 10 wt% of untreated CNC.

At the lower CNC contents (0.1 and 1 wt%), there was no great difference in the tan δ_c-values between the results for the filled and unfilled polymer, and the values were quite insensitive to the strain amplitude imposed. However, with 10 wt% CNC, the loss factor increased markedly with increasing strain amplitude, perhaps indicating a loss of adhesion between the CNC and the polymer or the break-up of possible CNC aggregates [29].

Figure 10 shows a graph similar to Fig. 9 for composites containing 10 wt% of the surface-treated as well as the untreated CNC. Measurements were
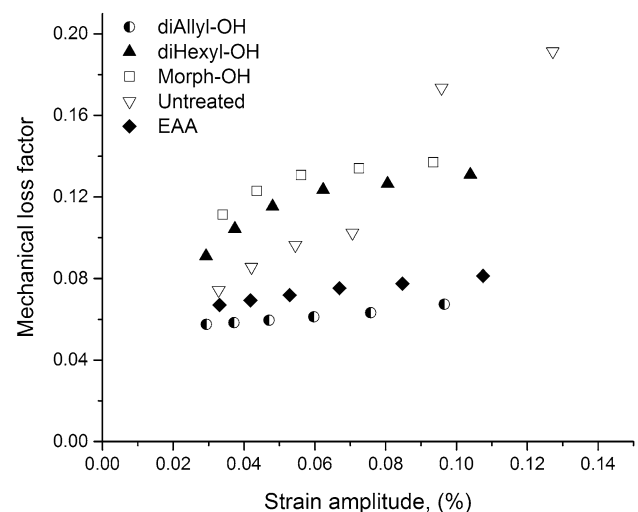

Figure 10 Mechanical loss factor as a function of the applied strain amplitude. The composites contained 10 wt% surface-treated CNC as well as 10 wt% untreated CNC.

also made on the composites containing the lower amounts of CNC, but the results are clearer at the highest CNC content. The surface treatment clearly affected the mechanical damping. In the case of CNC-Morph-OH and CNC-diHexyl-OH, the loss factor was higher than that of the composite containing the untreated CNC, at least at lower strain amplitudes. For both composites containing the treated nanocellulose, the loss factor was less sensitive to the strain amplitude than in the case of the composite based on the untreated CNC. The surface treatment may promote a rather flexible interphase region close to the CNC, which to some extent is in line with the yield behaviour of the composites. The composite containing 10 wt% CNC-diAllyl-OH exhibited the lowest tan δ_c-value (and a low dependence on the strain amplitude), clearly lower than that of the composite containing the untreated CNC. This may indicate a rather strong interphase region. This composite also exhibited the highest strength values with regard to the yield behaviour.

The composite containing 10 wt% CNC-diAllyl-OH actually exhibited lower tan δ_c-values than the unfilled EAA polymer. This may not be unrealistic if the adhesion between the nanocellulose and the polymer is sufficiently good, since CNC should exhibit a lower loss factor than the EAA. For example, for a paper sheet made of bleached sulphate pine pulp with a density of approximately 1000 kg/m^3, a tan δ_c-value close to 0.01 has been reported [38], whereas the value for the EAA polymer was in the range of 0.07 to 0.08. It is furthermore expected that nanocrystals should exhibit a lower mechanical loss factor than paper.

## Thermal transitions and crystallinity

Non-isothermal crystallisation of EAA can give a material which exhibits multiple endothermic melting peaks when the material is reheated [32], and ethylene–methacrylic acid copolymers show a similar behaviour [39]. This was also noted in the case of the composites used in the present work (Fig. 11). Multiple peaks can be associated with crystalline structures that differ in, for example, lamellae thickness and composition. Figure 11 shows the endotherms for the composite materials containing 10 wt% CNC, and a similar behaviour was observed at the lower CNC contents as well as with the unfilled EAA. The positions of the melting peaks were not markedly
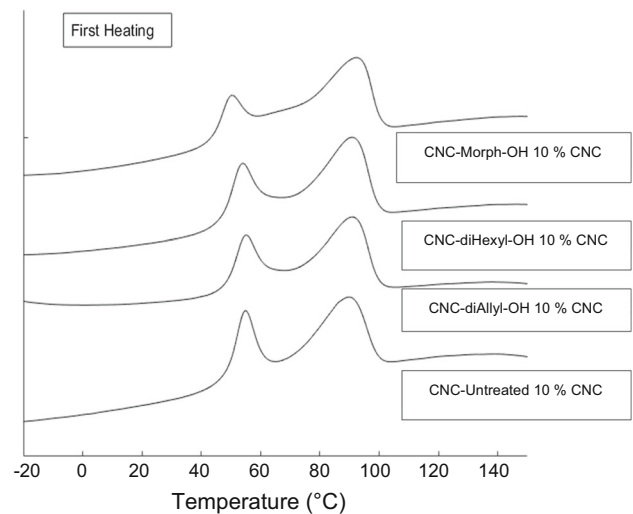
Figure 11 DSC endotherms for the composites containing surface-treated and untreated CNC (10 wt%).

affected by the amount of CNC in the composites, and they were similar to those of the unfilled EAA matrix (see also [32]). As reported by Venkatesh et al. [32], a second heating in the DSC equipment after cooling to − 20 °C resulted in a more distinct peak at approximately 88 °C at the expense of the intensity of the lower melting peak.

The total crystallinity corresponding to the multiple melting endotherms in Fig. 12 was calculated using Eq. (2). As shown in Fig. 12, the inclusion of CNC in the polymer matrix had only a marginal effect on the crystallinity. There was a slight tendency for the composites containing the surface-treated CNC to exhibit a higher crystallinity than the
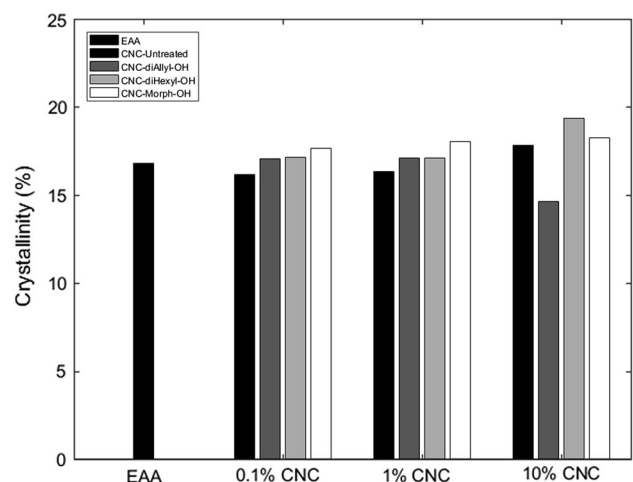
Figure 12 Total crystallinity of the unfilled EAA and the CNC-containing composites.

polymer reinforced with the untreated nanocrystals. It is evident that the improvements in mechanical properties, e.g. the modulus, when CNC is added to the matrix cannot be associated with a corresponding increase in crystallinity of the composites.

Conclusions

Hydroxyazetidinium salts were used to surface-modify CNC particles, and the grafting of the salts onto the sulphate ester groups of the CNC was confirmed by ζ-potential measurements and by the thermal degradation behaviour of the modified nanocrystals. In agreement with earlier studies on similar systems [23], the grafting improved the thermal stability of the CNC, i.e. the temperature for the onset of thermal degradation was raised by almost 100 °C.

The surface-modified CNC as well as the unmodified CNC were used as reinforcing elements in a matrix of an ethylene-based copolymer. Using a compression moulding procedure, it was possible to produce composite materials with well-dispersed CNC particles at concentrations up to 10 wt% CNC. The thermal stability of the composite material was not, however, markedly improved by the surface treatment of the nanocellulose. The reason for this was suggested to be associated with the alkaline character of the dispersions used when producing the composites resulting in a degrafting of the functional groups on the CNC surfaces at the high temperatures used for the TGA studies. Model experiments indicated, however, that such a degrafting did not take place at the lower temperatures used when manufacturing the composite materials. Further model experiments using a pH-neutralised mixture of the copolymer and a surface-modified CNC supported the hypothesis that the alkalinity influenced the thermal stability. In the case of a composite based on the neutralised system, the onset of thermal degradation was clearly shifted upwards to a higher temperature.

Addition of CNC to the EAA matrix had a strong effect on the mechanical behaviour of the composite materials. For example, the elastic modulus could in some systems be increased by a factor of three when 10 wt% CNC was added. Model calculations indicated such an improvement corresponding to an elastic modulus of the CNC of the order of

55–60 GPa. The surface treatment of the CNC appeared to mainly affect the yield behaviour and the ductility of the composite material. Measurements of the dynamic-mechanical loss factor indicated that the surface treatment had a clear effect on the properties of an interphase region between the CNC particles and the matrix. The effect on the mechanical properties of the composites is interpreted as being the result of interactions between the grafted groups and the polymer matrix and/or interactions between the grafted groups on different CNC entities.

The results obtained in this study are important since they indicate possible routes for the production of composites containing cellulosic reinforcing components with enhanced mechanical and thermal performance using conventional processing techniques such as extrusion and injection moulding.

References

[1] Berggren K, Klason C, Kubát J (1975) Spritzgiessen holzmehlhaltiger Thermoplaste. Kunststoffe 12(2):69–74

[2] Kokta BV, Chen R, Daneault C, Valade JL (1983) Use of wood fibers in thermoplastic composites. Polym Compos 4:229–232. https://doi.org/10.1002/pc.750040407

[3] Klason C, Kubát J, Strömvall H-E (1984) The efficiency of cellulosic fillers in common thermoplastics. Part 1. Filling without processing aids or coupling agents. Int J Polym Mater 10:159–187. https://doi.org/10.1080/00914038408080268

[4] Domininghaus H (1999) Plastics for engineers. Hanser, Munich

[5] Miao C, Hamad WY (2013) Cellulose reinforced polymer composites and nano-composites: a critical review. Cellulose 20:2221–2262. https://doi.org/10.1007/s10570-013-0007-3

[6] Pickering KL, Aruan Efendy MG, Le TM (2016) A review of recent developments in natural fibre composites and their mechanical performance. Compos A 83:98112. https://doi.org/10.1016/j.compositesa.2015.08.038

[7] Dalväg H, Klason C, Strömvall H-E (1985) The efficiency of cellulosic fillers in common thermoplastics. Part 1. Filling with processing aids and coupling agents. Int J Polym Mater 11:9–38. https://doi.org/10.1080/00914038508078651

[8] Trejo-O'Reilly J-A, Cavaille J-Y, Gandini A (1997) The surface chemical modification of cellulosic fibres in view of their use in composite materials. Cellulose 4:305–320. https://doi.org/10.1023/A:1018452310122

[9] George J, Sreekala MS, Thomas S (2001) A review on interface modification and characterization of natural fiber reinforced plastic composites. Polym Eng Sci 41:1471–1485. https://doi.org/10.1002/pen.10846

[10] Baiardo M, Frisoni G, Scandola M, Licciardello A (2002) Surface chemical modification of natural cellulose fibers. J Appl Polym Sci 83:38–45. https://doi.org/10.1002/app.2229

[11] Beck-Candanedo S, Roman M, Gray DG (2005) Effect of reaction conditions on the properties and behavior of wood cellulose nanocrystal suspensions. Biomacromol 6:1048–1054. https://doi.org/10.1021/bm049300p

[12] Boldizar A, Klason C, Kubát J, Näslund P, Sáha P (1987) Prehydrolyzed cellulose as reinforcing filler for thermoplastics. Int J Polym Mater 11:229–262. https://doi.org/10.1080/00914038708078665

[13] Favier V, Chanzy H, Cavaillé JY (1995) Polymer nanocomposites reinforced by cellulose whiskers. Macromolecules 28:6365–6367. https://doi.org/10.1021/ma00122a053

[14] Samir MASA, Alloin F, Sanches J-Y, Dufresne A (2004) Cellulose nanocrystals reinforced poly(oxyethylene). Polymer 45:4149–4157. https://doi.org/10.1016/j.polymer.2004.03094

[15] Xu X, Liu F, Jiang L, Zhu JY, Haagenson D, Wiesenborn DP (2013) Cellulose nanocrystals vs. cellulose nanofibrils: a comparative study on their microstructures and effects as polymer reinforcing agents. ACS Appl Mater Interfaces 5:2999–3009. https://doi.org/10.1021/am302624t

[16] Ansari F, Galland S, Johansson M, Plummer CJG, Berglund LA (2014) Cellulose nanofiber network for moisture stable, strong and ductile biocomposites and increased epoxy curing rate. Compos A 63:35–44. https://doi.org/10.1016/j.compositesa.2014.03.017

[17] Lee K-Y, Aitomäki Y, Berglund LA, Oksman K, Bismark A (2014) On the use of nanocellulose as reinforcement in polymer matrix composites. Compos Sci Technol 105:15–27. https://doi.org/10.1016/j.compscitech.2014.08.032

[18] Ansari F, Skrifvars M, Berglund L (2015) Nanostructured biocomposites based on unsaturated polyester resin and a cellulose nanofiber network. Compos Sci Technol 117:298–306. https://doi.org/10.1016/j.compscitech.2015.07.004

[19] Morelli CL, Belgacem MN, Branciforti MC, Salon MCB, Bras J, Bretas RES (2016) Nanocomposites of PBAT and cellulose nanocrystals modified by in situ polymerization and melt extrusion. Polym Eng Sci 56:1339–1348. https://doi.org/10.1002/pen.24367

[20] Moberg T, Tang H, Zhou Q, Rigdahl M (2016) Preparation and viscoelastic properties of composite fibres containing cellulose nanofibrils: formation of a coherent fibrillar network. J Nanomater. https://doi.org/10.1155/2016/9569236

[21] Roman M, Winter WT (2004) Effect of sulfate groups from sulfuric acid hydrolysis on the thermal degradation behavior of bacterial cellulose. Biomacromol 5:1671–1677. https://doi.org/10.1021/bm034519+

[22] Wang N, Ding E, Cheng R (2007) Thermal degradation behaviors of spherical cellulose nanocrystals with sulfate groups. Polymer 48:3486–3493. https://doi.org/10.1016/j.polymer.2007.03.062

[23] Sahlin K, Forsgren L, Moberg T, Bernin D, Rigdahl M, Westman G (2018) Surface treatment of cellulose nanocrystals (CNC): effects on dispersion rheology. Cellulose 25:331–345. https://doi.org/10.1007/s10570-017-1582-5

[24] Börjesson M, Sahlin K, Bernin D, Westman G (2018) Increased thermal stability of nanocellulose composites by functionalization of the sulfate groups on cellulose nanocrystals with azetidinium ions. J Appl Polym Sci. https://doi.org/10.1002/app.45963

[25] Ariño R, Boldizar A (2012) Processing and mechanical properties of thermoplastic composites based on cellulose fibers and ethylene-acrylic acid copolymer. Polym Eng Sci 52:1951–1957. https://doi.org/10.1002/pen.23134

[26] Hasani M, Cranston ED, Westman G, Gray DG (2008) Cationic surface functionalization of cellulose nanocrystals. Soft Matter 4:2238–2244. https://doi.org/10.1039/b806789a

[27] Moberg T, Sahlin K, Yao K, Geng S, Westman G, Zhou Q, Oksman K, Rigdahl M (2017) Rheological properties of nanocellulose suspensions: effects of fibril/particle dimensions and surface characteristics. Cellulose 24:2499–2510. https://doi.org/10.1007/s10570-017-1283-0

[28] Chattopadhyay S, Keul H, Moeller M (2012) Functional polymers bearing reactive azetidinium groups: synthesis and characterization. Macromol Chem Phys 213:500–512. https://doi.org/10.1002/macp.201100480

[29] Nielsen LE (1974) Mechanical properties of polymers and composites. vol 2, Marcel Dekker Inc, New York, pp 405–415; 422–429

[30] Kubát J, Rigdahl M, Welander M (1990) Characterization of interfacial interactions in high density polyetlylene filled with glass spheres using dynamic-mechanical analysis. J Appl Polym Sci 39:1527–1539. https://doi.org/10.1002/app.1990.070390711

[31] Brandrup J, Immergut E, Grulke E (1999) Polymer handbook, 4th edn. Wiley, Hoboken

[32] Venkatesh A, Thunberg J, Moberg T, Klingberg M, Hammar L, Peterson A, Müller C, Boldizar A (2018) Cellulose nanofibril-reinforced composites using aqueous dispersed ethylene-acrylic acid copolymer. Cellulose. https://doi.org/10.1007/s10570-018-1875-3

[33] Allen NS, Lo D, Salim MS, Jennings P (1990) Influence of amine structure on the post-cured photoyellowing of novel amine diacrylate terminated ultraviolet and electron beam cured coatings. Polym Degrad Stab 28:105–114. https://doi.org/10.1016/0141-3910(90)90055-C

[34] Xiao P, Shi S, Nie J (2008) Synthesis and characterization of copolymerizable one-component type II photoinitiators. Polym Adv Technol 19:1305–1310. https://doi.org/10.1002/pat.1132

[35] Matthews FL, Rawlings RD (1994) Composites materials: engineering and science. Chapman & Hall, London

[36] McCrum NG, Buckley CP, Bucknall CB (1997) Principles of polymer engineering, 2nd edn. Oxford Science Publications, Oxford

[37] Tanpichai S, Quero F, Nogi M, Yano H, Young RJ, Lindström T, Sampson WW, Eichorn SJ (2012) Effective Young's modulus of bacterial and microfibrillated cellulose fibrils in fibrous networks. Biomacromol 13:1340–1349. https://doi.org/10.1021/bm300042t

[38] Salmén L, Rigdahl M (1984) Dynamic mechanical properties of paper: effect of density and drying restraints. J Mater Sci 19:2955–2961. https://doi.org/10.1007/bf01026973

[39] Wakabayashi K, Register RA (2006) Morphological origin of the multistep relaxation behavior in semicrystalline ethylene/methacrylic ionomers. Macromolecules 39:1079–1086. https://doi.org/10.1021/ma052081v